Multimedia Tools and Applications
https://doi.org/10.1007/s11042-024-19140-9

Improved top-down attention phasmatodea population spiking neural network based multi crop recommendation framework

Chetan R[1,2] · D. V. Ashoka[3] · Ajay Prakash B[4]

Received: 26 October 2023 / Revised: 4 January 2024 / Accepted: 31 March 2024

Abstract
Modern agriculture refers to the contemporary practices, technologies and methods used in food production to meet the growing global demand for agricultural products. With increasing concerns about environmental degradation, soil health and resource depletion, there is an insistent need for agricultural practices that are both productive and sustainable. Multicropping mitigate the negative impacts of monoculture and reduce the reliance on synthetic inputs. This research introduces an innovative approach for multi-crop recommendation through the utilization of an integrated framework that combines advanced optimization techniques and neural networks like Enhanced top-down attention Spiking Neural Network (ETSNN). The proposed framework involves two main phases: the first phase focuses on classifying soils suitable for specific agro-ecological zones using an enhanced top-down attention spiking neural network. The second phase predicts multi-crop yields across different districts based on various environmental parameters using an Improved Phasmatodea population Evolutionary Algorithm (IPEA). Before classifying the crops feature selection takes place for the dataset by Enhanced Sea horse Optimization (ESO) method. The outputs from both phases are harmonized using a stacking-based fusion method. The developed user interface accepts real-time input for location-specific soil properties and provides crop recommendations that take into account both the input data and climate parameters. The proposed method attains 99.7% accuracy, 99.2% precision, 99% recall and 99.9% F1-score respectively.

Keywords Modern agriculture · Multicropping · Monoculture · Agro-ecological zone · Stacking based fusion

1 Introduction

Modern agricultural technology have introduced genetically enhanced crop varieties that produce larger quantities of crops per unit of land. Advanced technologies are integrated into various aspects of modern agriculture [1, 2]. This includes precision agriculture tools that use data, sensors and GPS to optimize planting, irrigation, fertilization, and pest

Extended author information available on the last page of the article

management for each part of a field. Monoculture farming is an agricultural practice where a single crop species is cultivated on a large scale in a specific area [3, 4]. This approach contrasts with polyculture, where multiple crops are grown together in the same space. Monoculture farming has been widely adopted in modern industrial agriculture due to its perceived efficiency and ease of management [5, 6]. Monoculture farming simplifies planting, maintenance and harvesting processes because only one type of crop is being grown. It leads to increase mechanization and streamline operations. Farmers be experts in growing a specific crop, maximize their knowledge and skills for optimal yield and quality [7, 8]. Few limitations of monoculture farming are, cultivating the same crop repeatedly results in the depletion of nutrients from the soil., leading to decreased soil fertility and potential erosion. Monocultures create ideal environments for pests and diseases to spread rapidly. A single pest or disease outbreak devastate an entire crop [9, 10]. Large-scale monoculture farming often replaces diverse ecosystems with uniform fields, leading to a reduction in local biodiversity and potential disruption of ecosystems.

Multicropping is also known as intercropping or polyculture farming. It is an agricultural strategy that involves cultivating multiple crop species in the same field simultaneously or in close proximity. This approach stands in contrast to monoculture farming, where a single crop dominates the landscape. Multicropping has gained attention for its potential to enhance agricultural sustainability, promote biodiversity and improve overall productivity. Multicropping reduce the risk of crop failure due to its inherent biological diversity. Pest and disease outbreaks that devastate a monoculture crop are less likely to spread rapidly in a diverse crop mix, as certain plants act as natural repellents or barriers to pests. Soil health is also positively impacted by multicropping. Different crop species improve soil structure, nutrient cycling and overall soil fertility.

The imperative to tackle the sustainability and productivity challenges of modern agriculture drives this research forward. In light of escalating environmental concerns and resource depletion, the research proposes an innovative approach that integrates advanced technologies to optimize crop selection. The ultimate goal is to empower farmers with precise recommendations grounded in soil classification, predicted yields, and environmental parameters. This, in turn, aims to foster sustainable practices and enhance overall agricultural outcomes.

The hypothesis posits that the proposed multi-crop recommendation system, leveraging enhanced top-down attention spiking neural networks and evolutionary algorithms, will significantly improve crop yield, soil health, and profitability. The system, by considering diverse factors, is expected to surpass traditional methods, offering tailored and data-driven recommendations. This contribution is envisioned to lead to a more sustainable and efficient agricultural ecosystem, addressing the contemporary challenges facing global agriculture.

1.1 Problem statement

The global agricultural sector, vital for sustenance and economic stability, faces challenges stemming from conventional monoculture farming practices. Issues such as soil degradation, diminished yield stability, and environmental impact are increasingly prevalent. To address these concerns and promote sustainable agriculture, an urgent need exists for effective multi-crop recommendation systems. These systems should guide farmers in selecting crops that optimize yield and resource utilization, overcoming challenges related to data

preprocessing, feature selection, and accurate crop classification, especially in specific agro-ecological zones.

In modern agriculture, the need for optimized multi-crop recommendation systems has grown significantly to enhance sustainability and productivity. This research paper introduces an integrated framework that leverages advanced computational techniques to address the challenge of multi-crop recommendation. By combining feature selection, neural network classification, evolutionary algorithms and stacking-based fusion, the proposed framework aims to provide accurate and context-specific recommendations for crop selection and yield prediction. The main contributions are,

- The image preprocessing module ensures that the input images are optimized and standardized for subsequent classification tasks aimed at determining the suitability of different crops for the specific agro-ecological zone.
- ETSNN suggests a focus on leveraging attention mechanisms and spiking neurons for improved soil image classification.
- ESO feature selection process enhances the efficiency and accuracy of crop classification for soil suitability, enabling the algorithm to emphasis on the most relevant and revealing aspects of the input soil images.
- ESHO's wave-based approach enables efficient exploration of the feature space, potentially discovering valuable feature combinations. It combines global and local search strategies, helping it escape local optima and find robust feature subsets.
- IPEA explore multiple solutions in parallel, which speed up the search for optimal classification models. It adapts the population over time, allowing it to converge toward better classification models.
- A multicrop recommendation framework harnesses technology and data to guide farmers toward diversified and ecologically friendly farming practices, addressing multiple challenges faced by modern agriculture and contributing to a more secure and sustainable food system.

Remaining part of this work is organized as follows: In Section 2, reviewed existing literature on diverse optimization and classification methods for soil and crop prediction. Section 3 delves into the proposed methodologies. Section 4 presents the results and discussions. Finally, Section 5 provides the conclusion and future work.

2 Literature survey

An inclusive literature survey was directed to collect insights from existing research papers in the fields of soil classification, crop prediction, and Crop Recommendation (CR). The objective of this survey was to understand the current state of knowledge, methodologies, and advancements in these critical areas of agriculture and precision farming.

Durai and Shamili in 2022 [11], explored into the application of Artificial Intelligent (AI) techniques in smart farming. Discusses the implementation of these technologies to create knowledgeable decisions about crop prediction. The authors highlight the role of data analytics in processing vast amounts of agricultural data, including soil and climatic parameters, to provide actionable insights for farmers. This work underscores the potential of machine learning in transforming traditional farming into a more efficient and data-driven practice. Thilakarathne N N et al. in 2022 [12], proposed a cloud-enabled CR

platform. This platform leverages AI algorithms to offer precision farming advice to farmers. The integration of cloud computing allows real-time access to data and recommendations, enabling farmers to make timely decisions. By employing a cloud-based approach, this research addresses the need for scalable and accessible solutions in modern agriculture. Madhuri J and Indiramma M in 2021 [13], presented an integrated CR system that employs Artificial Neural Networks (ANN). The system considers soil and climatic parameters to offer tailored crop suggestions. This study underscores the significance of incorporating multiple factors for accurate recommendations. By utilizing neural networks, the authors showcase the potential of complex data analysis in aiding farmers' decision-making processes. In line with the integration of the Internet of Things (IoT) in agriculture, Kiruthika S and Karthika D in 2023 [14], proposed an IoT-based professional CR function. This system utilizes a weight-based long-term memory approach to offer personalized crop advice. The authors emphasize the real-time data collection capabilities of IoT devices and the benefits of long-term memory for retaining historical farming data. Lanjewar and Gurav in 2022 [15], explores the use of Convolutional Neural Networks (CNNs) for classifying soil images. This study showcases the potential of deep learning in analyzing visual data related to soil composition. By accurately categorizing soil images, farmers and researchers gain insights into soil health and quality. The authors emphasize the non-invasive nature of image-based analysis and its potential to revolutionize soil assessment practices.

Uddin M and Hassan M R in 2022 [16], introduced a novel feature-based algorithm for soil type classification. Proposed an innovative approach to classifying soil types by leveraging distinctive features. It aims to enhance the accuracy of soil classification by utilizing these unique features. By employing this algorithm, the authors contribute to the field of soil science and classification methods. Dutta et al. in 2023 [17], presented an intriguing approach to soil classification using cat swarm with Fuzzy Cognitive Maps (FCM). This innovative method combines the concepts of cat swarm optimization and fuzzy cognitive maps to automate soil classification. By fusing these techniques, the authors offer a promising solution for accurate and automated soil classification, contributing to advancements in soil analysis and categorization. Kumar et al. in 2021 [18], introduced an automated soil prediction technique that employs the bag-of-features framework and the Chaotic Spider Monkey Optimization (CSMO) algorithm. Their research focuses on enhancing soil prediction accuracy by combining these two methodologies. This approach showcases the potential of integrating different algorithms for improved results in soil prediction applications. Barman U and Choudhury R.D in 2020 [19], contribute to the field of soil texture classification with their study utilizing a multi-class Support Vector Machine (SVM). The research focuses on accurately categorizing soil textures using this machine learning technique. By utilizing SVM, the authors aim to provide a reliable method for soil texture classification, which has implications for various agricultural and environmental applications. Kamath et al. in 2021 [20], addresses a crop yield forecasting using data mining techniques. Their research aims to predict crop yields based on data-driven methods. By employing data mining approaches, the authors explore ways to anticipate and forecast crop yields, which holds significance for agriculture and food production planning.

Gopi and Karthikeyan in 2023 [21], introduced an innovative approach for CR and yield prediction. Combined the Red Fox Optimization algorithm with an Ensemble of Recurrent Neural Networks (RFOERNN) to create a robust model. This approach leverages the Red Fox Optimization's ability to find optimal solutions and the RNN's capability to capture sequential data patterns. Munaganuri and Narasimha Rao in 2023 [22], presented the Capsule assisted stacked dilated Bi-LSTM (Cap-DiBiL) model. This automated model focuses

on predicting crop water requirements and providing suitable crop recommendations for agricultural practices. Cap-DiBiL's potential lies in optimizing water usage, reducing wastage, and ensuring the sustainability of crop production, all of which are vital aspects of modern agriculture. Gupta et al. in 2022 [23], introduced a comprehensive framework like Particle Swarm Optimization-SVM (PSO-SVM) for accurate crop yield prediction. This approach integrated machine learning techniques with feature selection methods, aiming to enhance the precision of crop yield predictions. By carefully selecting relevant features from the dataset, the model demonstrated improved performance in estimating crop yields. Table 1 lists the methods, objectives, limitations of reviewed research papers.

Numerous techniques have been suggested for crop recommendation framework. But the performance of existing approaches is not satisfactory. To overcome the limitations, some solutions essential to be put forward to fix these problems. This article aims to enhance agricultural decision-making, increase productivity and optimize resource utilization

3 Proposed methodology for multi crop recommendation framework

Agro-Ecological (AE) zone plays an essential role in deciding the crop to be cultivated in specific land areas. The proposed method aims to develop a multi crop recommendation frame work. There are many other crops that suitable for different agro-ecological zones. It's essential to consider specific factors such as temperature, rainfall and soil type. This article aims to enhance agricultural decision-making, increase productivity and optimize resource utilization.

Fig. 1 represents the proposed architecture of proposed approach. The input soil image data is preprocessed and classified using ETSNN method. ESO based feature selection is takes place for the data which collected from crop predict and crop recommendation dataset. Selected features are classified using IPEA approach. Finally, predicted soil and predicted features are get fused by using stacking based fusion technique.

3.1 First phase: soil image classification

The Image Preprocessing Module (IPM) technique [24] is applied to images collected from a soil image dataset. This technique involves precise classification of initial soil images to determine various characteristics, such as soil type and potential anomalies. The IPM approach remains consistent, storing images without specific features for testing purposes and images with relevant characteristics for training. Once deals with soil images, the IPM utilizes google vision to generate four coordinate points namely upper left, right, lower left and right for a region of interest within the initial image. These points are then employed to create a standardized square image.

Preprocess () function transforms the initial soil image into a preprocessed version. Retrieve an initial soil image and utilize google vision to obtain the four coordinate points. Calculate the four coordinate points based on the image. Verify that the points are not aligned with the corners of the image and that exactly four points are available.

Save Image () function manages the storage of the preprocessed soil image on the server. For training images, preprocess them using the Preprocess () function. After preprocessing, if a valid preprocessed image is obtained, it is stored in the training image directory. If no preprocessed image is produced, the system decides that the processed image isn't appropriate for training and doesn't store it on the server. IPM aims to accurately classify and

Table 1 Summary of existing methods

References	Methods	Objectives	Limitations
[11]	AI techniques	Enhance smart farming practices using AI	There is a potential dependency on data quality
[12]	Cloud-enabled platform with machine learning algorithms	Develop a crop recommendation platform for precision farming	Dependence on stable internet connectivity. Privacy and security concerns with cloud data
[13]	ANN	Create an integrated CR system	Complexity of neural network training
[14]	Weight-based long-term memory approach	Design a professional crop recommendation system	Dependence on IoT infrastructure
[15]	CNN	Perform classifications of soil images using CNNs	Depend more image quality and diversity
[16]	Novel feature-based algorithm	Develop an innovative algorithm for soil classification	Potential dependency on data quality
[17]	FCM	Create an automated soil classification method	Complexity in combining different methodologies
[18]	Bag-of-features and CSMO	Develop an automated soil prediction approach	Generalization across different soil conditions
[19]	Multi-class support vector machine	Perform soil texture classification using SVM	Challenges in handling multi-class classification
[20]	Data mining	Focus on forecasting crop yields using data mining	Performance variation is there for different crop types
[21]	RFOERNN	To enhance accuracy in crop recommendation and yield prediction. -	Applicability to various crop types and regions may vary
[22]	Cap-DiBiL	To recommend suitable crops for specific agricultural conditions	Relies on the availability of accurate weather and soil data
[23]	PSO-SVM	To provide valuable insights for farmers and policymakers	Generalizability across diverse crops and regions may vary

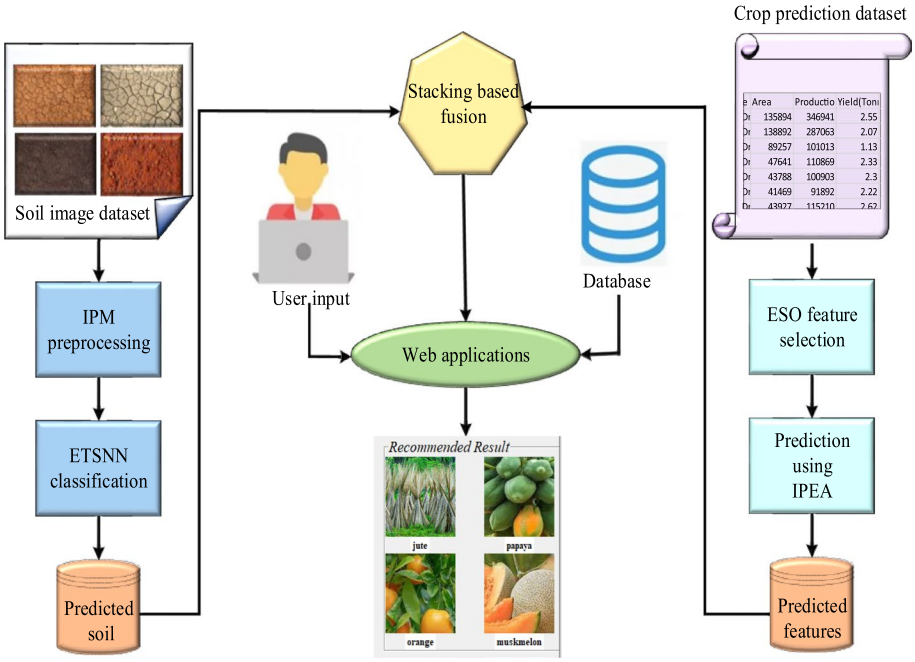

Fig. 1 Proposed architecture

process soil images, segregating them into testing and training datasets based on their characteristics. The preprocessed soil image is classified by using ETSNN approach.

3.1.1 Enhanced top-down attention spiking neural network for classification

An Enhanced Top-Down Attention Spiking Neural Network is an advanced neural network architecture that combines spiking neurons with top-down attention mechanisms. While applying ETSNN for classification it first extract features from soil such as color information, shape features, size area, and pattern analysis after preprocessing. These features facilitate autonomous soil classification, allowing the network to learn and categorize soil types based on the extracted image characteristics. The ETSNN method inspired by the top-down attention mechanisms observed in the human perceptual system. The network is designed to selectively focus on relevant regions or features in soil images to aid in classification [25]. Fig. 2 represents the classified soil image. Input soil is predicted like soil type ("red soil") and its score. In the realm of soil classification, the utilization of histograms as a visualization and analytical tool offer profound insights into the distribution of soil properties. A particularly intriguing phenomenon that arise in soil classification is the emergence of a bi-modal histogram.

The backbone of the network would likely be a Spiking Neural Network (SNN). SNNs are suitable for processing spatiotemporal data, making them potentially well-suited for analyzing soil images that may have both spatial and temporal characteristics. The SNN serve as a feature extractor, converting soil image data into a spatiotemporal representation that capture meaningful patterns. Eqn. (1) expresses the function of the feature extractor.

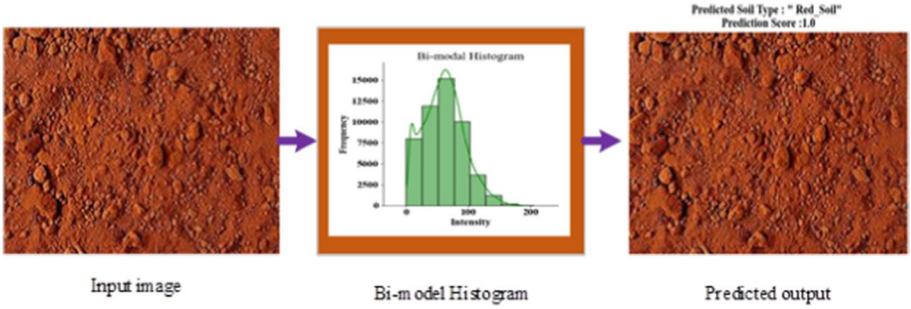

Fig. 2 Classified image of soil

$$G(s) = C\left(Z(s) \times N_m, \theta_C, h_C\right) \tag{1}$$

where, $G(s)$ represents the time varying pixels, $C()$ represents the feature extractor, $Z(s)$ represents the input feature, N_m represents the attention map, θ_C represents the learnable parameters, h_C represents the original value of the state variable. $G(s)$ is subsequently input into the classifier to provide predictions, which could include recognition task categories. To enhance prediction reliability $G_E(s)$, the classifier's outputs at every sampling time are consolidated and then undergo processing by a trainable decoder to produce the better outcome. Equation (2) formulate the following process.

$$\begin{cases} G_E(s) = E\left(G(s), \theta_E, h_E\right) \\ Z = k_E^S\left[G_E\left(S_e\right)^S, G_E\left(2S_e\right)^S, \ldots \ldots G_e\left(LS_e\right)^S\right]^S + b_E \end{cases} \tag{2}$$

where, z represents the ultimate recognition prediction. Likewise, θ_E represents the trainable parameters, s denotes iterations and h_E signifies the initial state variables of $E()$. k_E and b_E are the parameters specific to the linear decoder. S_e stands for the sampling interval, G_E denoted as image and L corresponds to the number of samplings during inference. For practical use, a commonly accepted setting involves S_e being configured as 1 ms. Consequently, L is determined by the duration of the input images.

To implement top-down attention, ANN component included in the architecture. ANN produce attention maps using the features extracted from the SNN. These attention maps would guide the SNN's focus, allowing it to attend to specific regions or features in the soil images that are most informative for classification. The ETSNN would likely employ a closed-loop inference process. This means that the attention mechanism modulates the behavior of spiking neural network, influencing its processing of soil images to ensure more reliable and context-aware classification.

The model is trained using labeled soil image data, where the goal is to optimize the SNN's feature extraction and the ANN's attention generation components simultaneously. Training could involve loss functions that encourage both accurate classification and the generation of meaningful attention maps. As the foundation of the (Hybrid Top-Down Attention) HTDA model, the feedforward SNN assumes a pivotal role in processing sensory inputs. SNNs exhibit intrinsic temporal dynamics, engage in sparse computation and respond to events, rendering them well-suited for handling spatiotemporal information. Within the HTDA model, choose the widely-adopted Leaky integrate-and-Fire (LIF) model for the SNNs. The LIF model offers ease of implementation and aligns reasonably

well with biological plausibility. Importantly, it's worth noting that the HTDA model maintains a degree of neutrality towards neuronal models and is not confined exclusively to the LIF model. Eqn. (3) describing the membrane potential of the LIF model.

$$\tau \frac{du(s)}{dt} = -\left(u(s) - u_{reset}\right) + WI(s) \tag{3}$$

where, $u(s)$ represents the membrane potential, and u_{reset} denotes the reset potential. τ signifies the time continuous, and W corresponds to the membrane resistance. Additionally, $I(s)$ encompasses the afferent neuron current, encompassing bias currents and pre-synaptic inputs.

The model would be trained using labeled soil image data, where the goal is to optimize the SNN's feature extraction and the ANN's attention generation components simultaneously. Training could involve loss functions that encourage both accurate classification and the generation of meaningful attention maps. The overall minimization goal is expressed in Eqn. (4).

$$L = \beta L_E + (1 + \beta) L_N \tag{4}$$

where, L_E signifies the loss relating to object recognition, while L_N pertains to the loss related to the generation of the attention map. The parameter β serves as a hyper parameter that fine-tunes the weighting between these two terms. The loss L_E instantiate using the softmax cross-entropy loss. By incorporating top-down attention mechanisms, the HTDA-SNN gain a contextual understanding of soil images, focusing on relevant areas and features for classification. Also leads to more accurate predictions. Spiking Neural Networks excel at handling temporal data and event-driven updates, it is advantageous for soil images that exhibit dynamic changes over time.

3.2 Second phase: text classification

The classification of crops is described in this section. Initially, the input data is collected from crop prediction and crop recommendation.csv file and select the features by using ESO method. After selecting the features PPE based classification takes place.

3.2.1 Enhanced sea horse optimization for feature selection

The collected data is preprocessed and to enhance the feature selection use a technique called Enhanced Sea horse Optimization (ESO) [26]. It aims to optimize feature subsets to enhance the performance of AI models by analyzing the most informative and relevant attributes. This algorithm is based on the behavior of sea horses in nature, including their movement patterns, predation habits and breeding activities. The ESO algorithm consists of three main components: mobility, predation, and breeding.

The mobility behavior of the sea horse involves spiraling movements around algal stems due to marine vortices. This is simulated to achieve exploration through brownian motion. In predation behavior, sea horses leverage their unique head shape to stealthily approach prey with high success rates. Breeding occurs after mobility and predation, where male and female sea horses randomly form new generations, passing down advantageous traits. The ESO algorithm is divided into four phases: initialization, mobility, predation and breeding behavior.

Initialization phase The initialization phase involves generating an initial population of sea horses, each representing a potential solution in the problem's search space. Eqn. (5) for generating individuals within specified bounds are provided.

$$T = \begin{bmatrix} z_1^1 & \bullet & \bullet & \bullet & z_1^H \\ \bullet & \bullet & & & \bullet \\ \bullet & & \bullet & & \bullet \\ \bullet & & & \bullet & \bullet \\ z_q^1 & \bullet & \bullet & \bullet & z_q^H \end{bmatrix} \tag{5}$$

where, z_1 represents the initial population and z_q^H represents the maximum population count with the H iteration.

Movement behavior phase Sea horses exhibit various movement patterns during their motion, approximately use a normal distributed random distribution (0, 1). The algorithm balances exploitation and exploration by considering a cut-off point at $r_1 = 0$. When r_1 is on the right side of the cut-off, local exploitation occurs, while on the left side, global search is prioritized.

- ***Step 1 (Exploration—Brownian Motion):*** When r_1 is on the right side, sea horses simulate their spiral movement in alignment with the ocean vortex. They follow the direction of the best solution Z_{best} and employ the Levy flight model for movement step size. This helps them explore distant spots and prevents over-localization. A new position for a sea horse is generated using an Eq. (6) involving three-dimensional coordinates and logarithmic spiral constants $z_{new}^1(s+1)$.

$$Z_{new}^1(s+1) = Z_j(s) + l(\lambda)\Big(\big(Z_{best}(s) - Z_j(s)\big) * u * v * w + Z_{best}(s)\Big)$$
$$s.t\begin{cases} u = q * \cos(\theta) \\ v = q * \sin(\theta) \\ w = q * \theta \\ q = a * h^{\theta v} \end{cases} \tag{6}$$

where, $Z_j(s)$ denotes updated population with s, $l(\lambda)$ denotes learnable parameter,*u, v and w* represent positions in three-dimensional space. These coordinates play a crucial role in updating the search agents' position. q denoted as length of the stems, h is determined by logarithmic spiral constants a and v. These constants are both set to 0.05. The value of θ is selected randomly from the range between 0 and 2π. The calculation of the Levy flight distribution function, represented as$l(x)$, is performed using Eq. (7).

$$l(x) = t * \frac{\omega * \sigma}{|f|^{\frac{1}{\lambda}}} \tag{7}$$

where, ω and f represent randomly generated positive numbers within the range of 0 to 1. The constant t holds a value of 0.01 and λ takes on a random value between 0 and 2. λ is assigned a value of 1.5. Equation (8) shows the expressions of σ.

$$\sigma = \left(\frac{\Gamma(1+\lambda) * \sin\left(\frac{\pi\lambda}{2}\right)}{\Gamma\left(\frac{1+\lambda}{2}\right) * \lambda * 2^{\left(\frac{\lambda-1}{2}\right)}} \right) \tag{8}$$

- ***Step 2 (Exploration—Brownian Motion):*** If r_1 is on the left side, sea horses simulate brownian motion due to ocean waves. This drift-like behavior aids in exploring the search space more efficiently. Equation (9) is the mathematical formula for this scenario.

$$\begin{gathered} Z^1_{new}(s+1) = Z_j(s) + rand * i * \beta_s * \left(Z_j(s) - \beta_j * Z_{best}\right) \\ s.t\left\{ \beta_s = \frac{1}{\sqrt{2\pi}} \exp\left(-\frac{z^2}{2}\right) \right. \end{gathered} \tag{9}$$

  where, the symbol i represents a fixed coefficient of 0.05 and j represents the iterations. The coefficient for the random walk of Brownian motion is indicated as β. These two factors merged to calculate the updated position of the seahorse during the s^{th} iteration. Equation (10) is the formula to calculate the updated position.

$$Z^1_{new}(s+1) = \begin{cases} Z^1_{new}(s+1) = Z_j(s) + l(\lambda)\left(\left(Z_{best}(s) - Z_j(t)\right) * u * v * w + Z_{best}(s)\right), r_1 > 0 \\ Z_j(s) + rand * i * \beta_S * \left(Z_j(s) - \beta_j * Z_{best}\right) \ , r_1 \le 0 \end{cases} \tag{10}$$

Predation behavior phase This phase simulates the sea horse's feeding habits on small organisms. A random number r2 is generated to determine success or failure in predation, with r2 set at a critical value of 0.1. *Success Case:* If r2 > 0.1, predation is successful. The sea horse approaches the target (best solution) and captures it, utilizing the target's information to enhance exploitation. *Failure Case:* If r2 ≤ 0.1, predation fails. The sea horse responds with a reversed motion, implying continue exploring the region. This behavior helps the algorithm to avoid local extrema and continue searching. The predation behavior is represented mathematically using an Eqn. (11).

$$Z^1_{new}(s+1) = \begin{cases} \alpha * \left(Z_{best} - rand * Z^1_{new}(s)\right) + (1-\alpha) * Z_{best} \ \ if r_2 > 0.1 \\ (1-\alpha) * \left(Z^1_{new}(s) - rand * Z_{best}\right) + \alpha * Z_{best}(s) \ \ if r_2 \le 0.1 \end{cases} \tag{11}$$

where, r_2 is a randomly chosen integer within the range of [0, 1], and $Z^1_{new}(s)$ signifies the updated position of the seahorse after its movement during the s^{th} iteration.

Breeding behavior phase The population is divided into two groups males and females based on their fitness levels. In sea horses, only males participate in breeding. To support this reproductive process, the ESO algorithm chooses the top half of the population with the highest fitness scores as fathers, while the remaining half becomes mothers. This division, outlined in Eqn. (12), prevents excessive concentration of new solutions in one area and facilitates the inheritance of advantageous traits from both parents to the succeeding generation.

$$\begin{cases} father = Z^2_{sort}\left(1 : \frac{q}{2}\right) \\ mother = Z^2_{sort}\left(\frac{q}{2} + 1 : q\right) \end{cases} \tag{12}$$

where, q represents the positive values; all the updated positions denoted as Z^2_{new} are arranged in ascending order based on their fitness values, and this ordered collection is referred to as Z^2_{sort}. The groups corresponding to female and male populations are symbolized by fathers and mothers.

To achieve this, random mating occurs between the male and female groups, leading to the birth of new offspring. To maintain efficiency, the SHO approach assumes that every pair of sea horse produces a single child, which is expressed in Eqn. (13). This approach ensures a controlled and streamlined execution of the algorithm while allowing for the creation of the next generation with the combined genetic features of both parents.

$$Z_j^{offspring} = r_3 Z_j^{father} + \left(1 - r_3\right) Z_j^{mother} \tag{13}$$

where, r_3 is a randomly selected integer from the range [0, 1]. An integer j is picked from the positive values within the interval $[1, {}^{q}\!/_{2}]$. The male and female members chosen at random are denoted as Z_j^{father} and Z_j^{mother}, respectively. Features are selected optimally based on the behavior of ESO. Selected features are classified by using the method IPEA.

3.2.2 Improved phasmatodean population evolutionary algorithm for prediction

IPEA is a metaheuristic optimization algorithm inspired by the behavior of stick insects (phasmatodeans) in the natural world. It falls under the category of nature-inspired algorithms, which are used to solve complex optimization problems. The IPEA algorithm is designed to find optimal or near-optimal solutions to various optimization problems. The selected features are then predicted using the IPEA [27]. Fig. 3 shows the flow chart of IPEA algorithm.It is described with three main stages: initialization, population update, and selection of the population.

Initialization stage In this stage, an $Mq \times c$ matrix z is randomly initialized, where each element z_j represents a population. Each population has attributes: population size q_j and growth rate b_j. The initial size is $q_j = \frac{1}{Mq}$, and initial growth rate is $b_j = 1.1$. The population evolution trend h_j is initially set to 0. The fitness value is calculated by using the Eq. (14), and the global optimal solution v_{best} is tracked. A historical global optimal solution matrix D is created to guide updates. D stores the k best solutions, where $k = [\log(Mq)] + 1$.

$$F(y,t,h,r) = w_1 y - w_2\left(\left|t - t_{opt}\right|\right) - w_3\left(\left|h - h_{opt}\right|\right) - w_4\left(\left|r - r_{opt}\right|\right) \tag{14}$$

where, $F(y,t,h,r)$ denotes fitness function of yield(crop), temperature, humidity and rainfall. $w_1, w_2, w_3 and w_4$ are the tuning parameters.

Population update stage The s^{th} updated population z_j^s is calculated. Equation (15) is the formula for updating the $s+1^{th}$ population.

$$z_j^{s+1} = z_j^s + h_j \tag{15}$$

After update the population, it is necessary to recompute the fitness value and make updates to both the v_{best} and D.

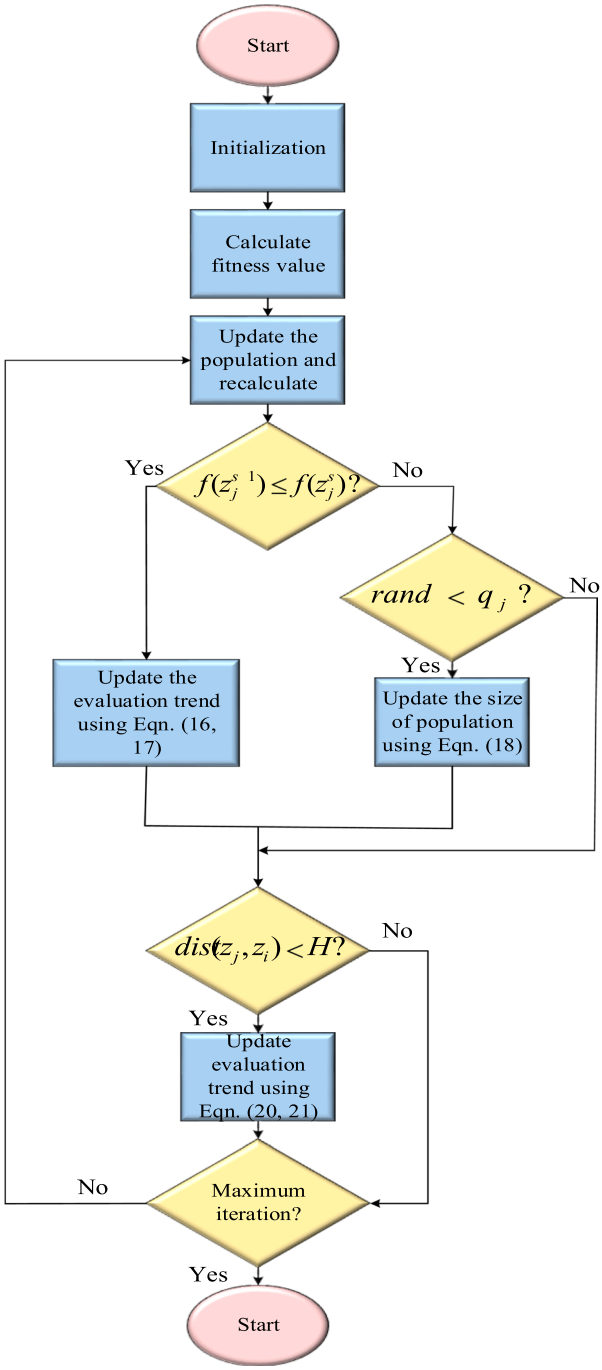

Fig. 3 Flow chart for IPEA method

Selection of population evolution trend stage Three cases are considered. First, if $f\left(z_j^{s+1}\right) \leq f\left(z_j^s\right)$ equations are used to update q_j and h_j. Equation (16) and (17) are used to update the population.

$$q_j^{s+1} = b_j^{s+1} q_j^s \left(1 - q_j^s\right) \tag{16}$$

$$h_j^{s+1} = \left(1 - q_j^{s+1}\right)\left[\left(z_{j,D}^s - z_j^s\right) \bullet l\right] + q_j^{s+1}\left(h_j^s + n\right) \tag{17}$$

where, n represents the mutual factor; l represents the impact factor. For the second case, if $f\left(z_j^{s+1}\right) > f\left(z_j^s\right)$, there is a probability of accepting` the update using the random method. If $rand < q_j$, the update is accepted and Eq. (18) is used to update h_j.

$$h_j^{s+1} = rand \bullet \left(z_{j,D}^s - z_j^s\right) + st \bullet A \tag{18}$$

where, A represents the randomly generated population matrix. The third case involves competition among populations based on a defined threshold H. Eqn. (19) shows the formula to define threshold. Eqn. (20) and (21) are used to update pi and ei.

$$H = 0.1 \times (W - O)\frac{Max_{gen} + 1 - s}{max\_gen} \tag{19}$$

$$q_j^{s+1} = q_j^s + b_j^s q_j^s \left(1 - q_j^s - \frac{f\left(z_j^s\right)}{f\left(z_j^s\right)} q_j^s\right) \tag{20}$$

$$h_j^{s+1} = h_j^s + \frac{f\left(z_j^s\right) - f\left(z_j^s\right)}{f\left(z_j^s\right)}\left(z_j^s - z_j^s\right) \tag{21}$$

IPEA involves maintaining populations, updating attributes and making probabilistic decisions based on fitness values and competition among populations. By using these techniques, the selected features are predicting the crops which are grown in the selected area, district, its temperature and fertility levels. Finally, concatenate the output of ETSNN and IPEA prediction by using stacking based fusion approach.

3.3 Third phase: stacking-based fusion for multicrop recommendation

The fusion approach through stacking modeling, in the context of soil image and crop prediction, begins by partitioning the initial feature dataset into multiple sub-datasets. Each of these sub-datasets is subsequently input into individual base learners within the first-level prediction model. These base learners generate their respective prediction outcomes. The essence of the stacking model fusion method lies in its ability to enhance overall prediction

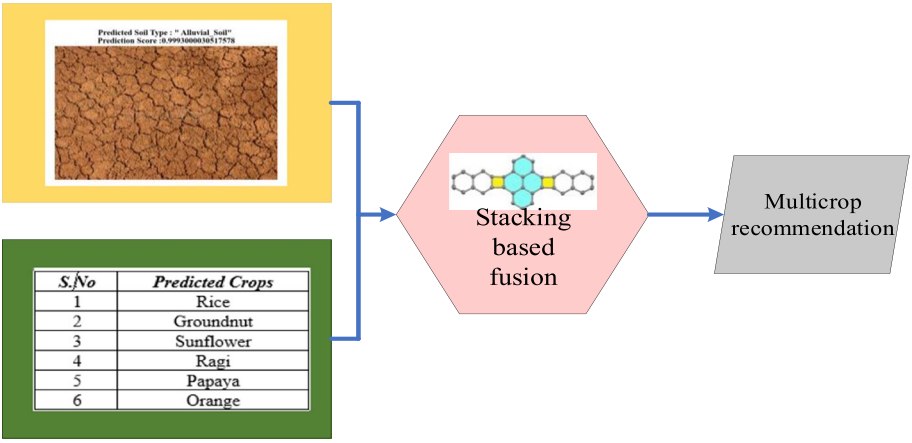

Fig. 4 Flow of stacking based recommendation process

accuracy by amalgamating the output results from various models. Fig. 4 represents the flow of stacking based recommendation process.

The initial dataset is segmented and apportioned into training and testing sets following a predetermined ratio, during the initial phase. Appropriate base learners are meticulously chosen to be trained on the training set through cross-validation. Upon completing the training process, each base learner performs predictions on both the validation and test sets. It's vital to identify machine learning models that exhibit relatively strong prediction performance, ensuring a diverse set of models.

In the subsequent phase, the prediction results from these base learners serve as the feature data for training and making predictions using the meta-learner. The meta-learner takes the features obtained in the prior stage and pairs them with the labels from the original training set to construct the model, ultimately yielding the final stacking model prediction results.

This approach entails acquiring two sets of predictions derived from two distinct integrated model algorithms with high prediction accuracy, which serve as the base learners. These two sets, along with a third set of predictions, are incorporated into the second layer by employing a meta-learner. The chosen meta-learner is then trained to form a bagging model, culminating in the ultimate prediction results. This process allows for a refined and more accurate prediction outcome, specifically tailored for the context of soil image and crop prediction.

4 Results and discussions

In this research process, python is the programming environment for conducting image processing experiments. The experiments is executed on a personal computer equipped with a robust hardware configuration, featuring a 3.40 GHz Intel Core i7-6700 CPU and 16GB of RAM. These hardware specifications provided plenty computational power to handle the tasks effectively.

To ensure a comprehensive evaluation of the algorithms and models, systematically divided the prepared databases into two distinct sets: a training set, encompassing 80% of

Table 2 Details about experimental setup

Configuration parameters	Value
OS	Windows 10 Pro
OS build	19,045.2965
Python version	Python 3.10.9
Datasets	CR, CR—analysis, CR—classification
Feature selection algorithm	GENGSO
Installed Ram	16.0 GB(15.8 GB usable)

the entire database, and a separate test set comprising the remaining 20%. This partitioning strategy is employed to facilitate rigorous testing and validation of methodologies. Table 2 encapsulates essential details regarding experimental setup, encompassing particulars related to the operating system, dataset composition, and algorithm configurations.

The soil image dataset comprises 903 images representing four distinct soil types (alluvial, black, clay, and red). The dataset was split into training and validation sets. Image augmentation techniques were applied to enhance the dataset, after which models were trained using these augmented images. The crop recommendation dataset contains the variables phosphorus (P), nitrogen (N), potassium (K), temperature, humidity, pH, precipitation, and label. The crop prediction dataset encompasses a diverse range of climatic and soil-related features that impact crop growth, facilitating the analysis and prediction of potential crop outcomes across various seasons. This dataset includes, *Temperature:* Average temperature in degrees Celsius, depicting regional climatic conditions. *Humidity:* Relative humidity expressed as a percentage, indicating atmospheric moisture. *pH:* Soil pH value, reflecting soil acidity or alkalinity. *Water Availability:* A metric representing soil moisture or water accessibility for plants. *Season:* A categorical feature denoting the recorded season, offering insights into the annual climate cycle. *Label:* Crop label indicating the cultivated crop type. Crops in the dataset include blackgram, chickpea, cotton, jute, kidneybeans, lentil, maize, mothbeans, mungbean, muskmelon, pigeonpeas, rice, and watermelon.

4.1 Results related to soil classification

The method ETSNN for soil classification has yielded promising results, demonstrating its effectiveness in accurately categorizing soil types based on image data. Figs. 5 (a) and (b) represents the classification of various images from soil image dataset. The input image is collected from soil image dataset (https://www.kaggle.com/datasets/atharvaingle/crop-recommendation-dataset).

The predicted soils are alluvial soil with the score 0.9993, black soil with the score 1, clay soil with the score 0.999899 and the red soil with the score 1. The bio model histogram for each soil is mentioned graphically with the frequency and intensity value. In evaluating the performance of soil classification model using the ETSNN, evaluated with comprehensive assessments based on several key metrics. These metrics provide a comprehensive understanding of the model's classification accuracy and its ability to discriminate between different soil types.

Fig. 6 shows the obtained accuracy of classified soil. Accuracy measures the overall correctness of soil classification. It quantifies the proportion of correctly classified soil samples out of the total samples in the dataset. ETSNN model achieved an impressive

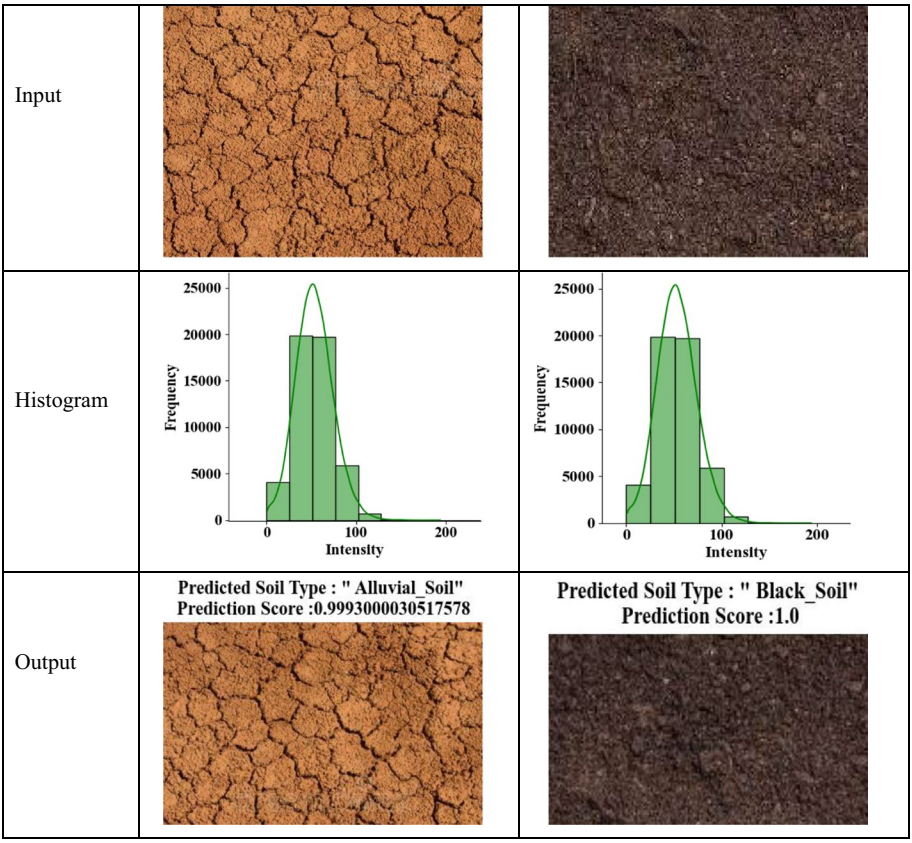

(a) Predicted soil images of Alluvial and Black soil

Fig. 5 **a** Predicted soil images of Alluvial and Black soil. **b** Classification of various images like clay and red soil from soil image dataset

accuracy of 98.94%, 98.4%, 98.4% and 98.94% in classifying soil types. Fig. 7 shows the obtained precision of classified soil. Precision assesses the model's ability to correctly classify soil samples within a specific category. It calculates the ratio of true positive predictions to the total predicted positives. ETSNN model exhibited a precision score of 97.87%, 97.87%, 95.83% and 97.83% for soil classification.

Fig. 8 shows the obtained recall value of classified soil. It calculates the ratio of true positives to the total actual positives. ETSNN model demonstrated a recall score of 97.87%, 95.83%, 97.87% and 97.83% for soil classification. Fig. 8 shows the obtained specificity of classified soil. It calculates the ratio of true negatives to the total actual negatives. ETSNN exhibited a specificity score of 99.29%, 99.29, 98.58% and 98.58% in distinguishing soils outside the target class.

Figs. 9 and 10 shows the obtained F1-score and specificity value for classified soil. These metrics collectively demonstrate the robustness and accuracy of our ETSNN based soil classification model. Its high accuracy, coupled with strong precision, recall, specificity, and F1 -score, affirms its effectiveness in classifying soil types accurately and reliably.

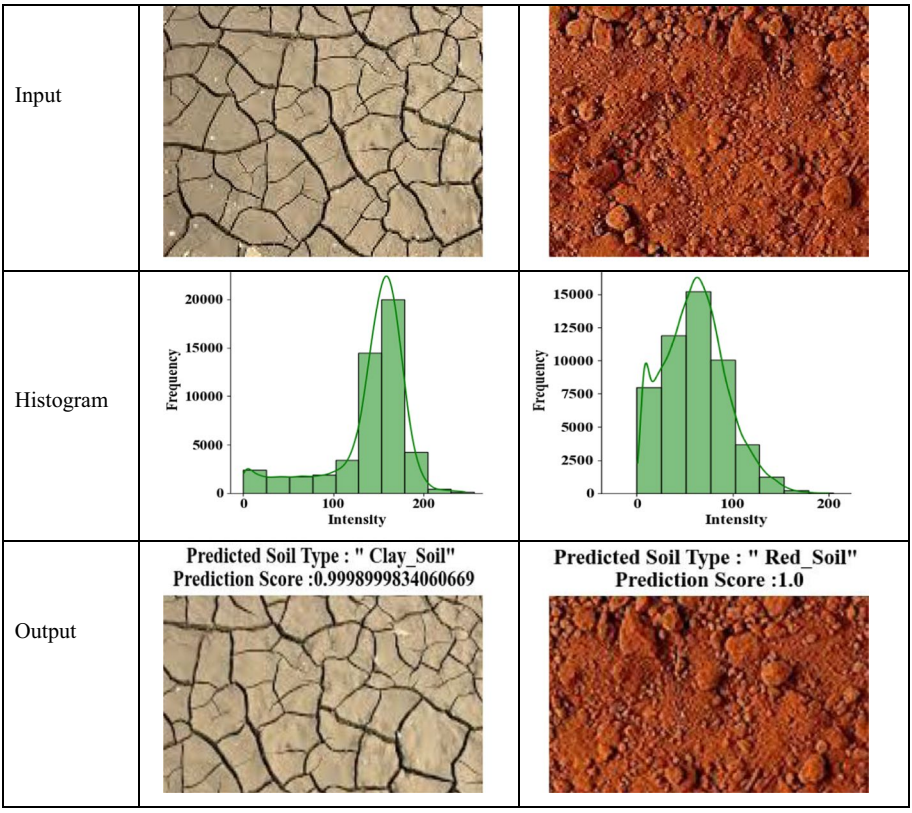

(b) Classification of various images like clay and red soil from soil image dataset

Fig. 5 (continued)

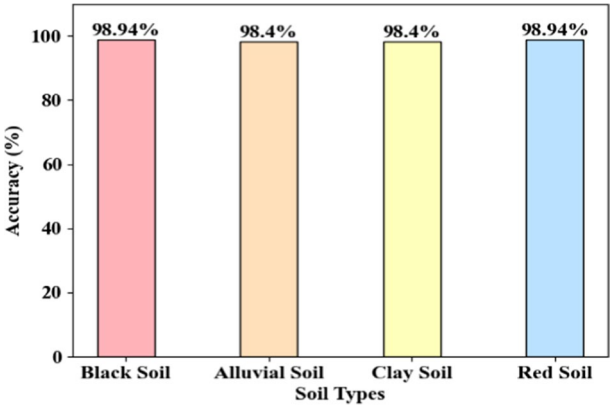

Fig. 6 Accuracy of classified soil

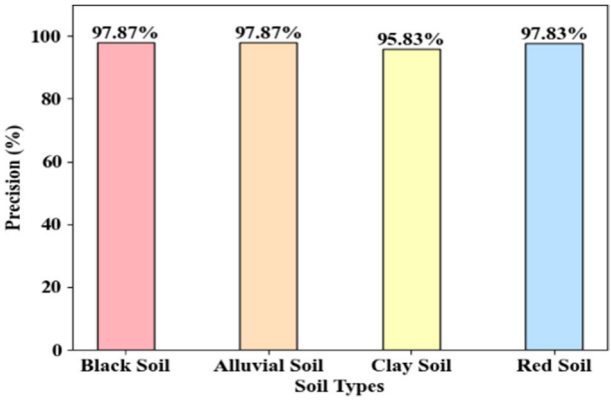

Fig. 7 Precision of classified soil

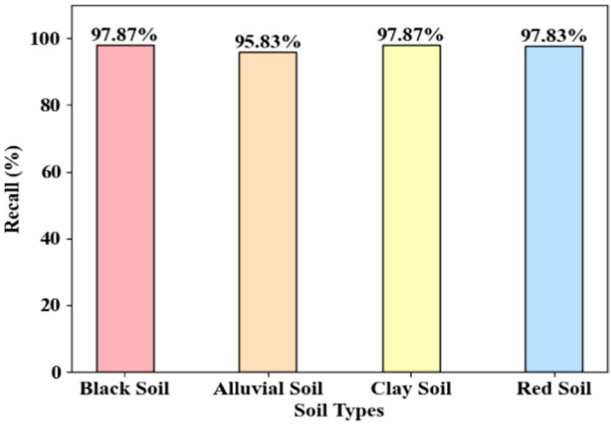

Fig. 8 Recall of classified soil

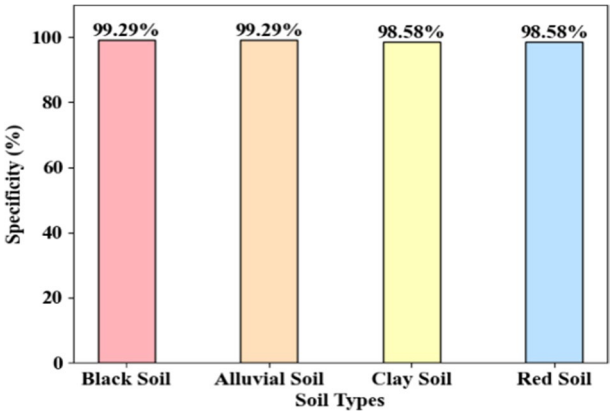

Fig. 9 Specificity of classified soil

After training soil classification model using ETSNN architecture, for a total of 200 epoch obtained highly promising results. Figs. 11 (a) and (b) represents the accuracy and loss values of soil classification during training. ETSNN model achieved an F1 -score of

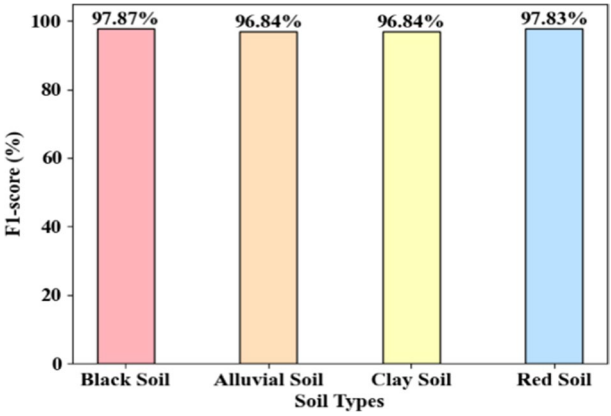

Fig. 10 F1-score of classified soil

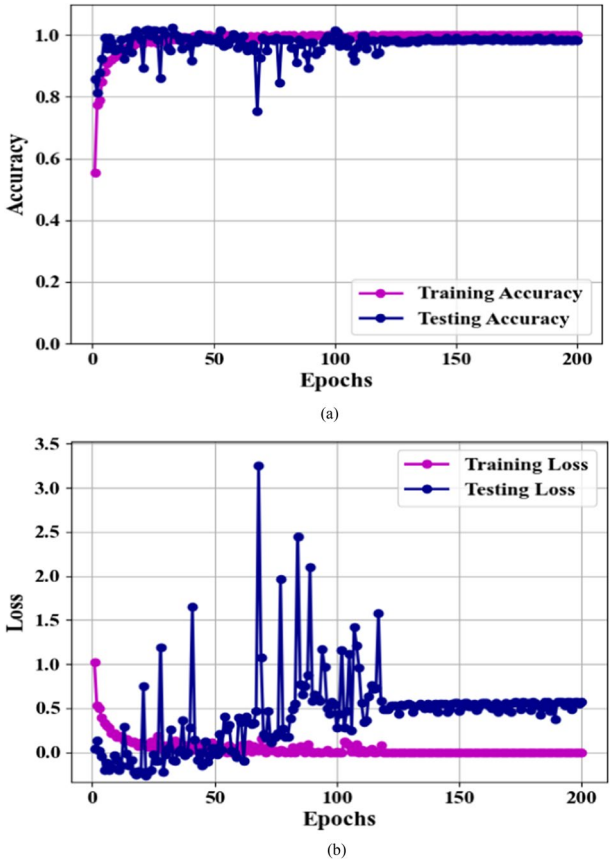

Fig. 11 **a** Accuracy and **b** Loss for classified soil with various epoch

97.87%, 96.84%, 96.84% and 97.83%, reflecting its ability to balance precision and recall effectively.

The trained ETSNN model achieved an outstanding accuracy of 99%, signifying that it appropriately classified 99% of the soil samples in the evaluation dataset. This unique

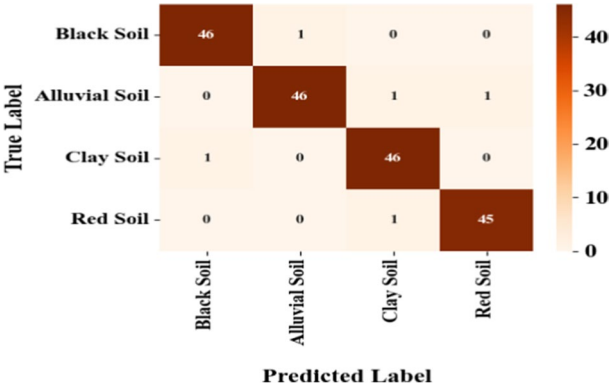

Fig. 12 Confusion matrix for classified soil image

Table 3 Performance evaluation of classified soil images

Performance evaluation	IPEA approach
Accuracy (%)	98.67
Precision (%)	97.34
Recall (%)	97.34
Specificity (%)	99.11
F1-score (%)	97.34
MAE (%)	0.0372
MSE (%)	0.0585
RMSE (%)	0.2418

accuracy emphasizes the model's proficiency in distinguishing between different soil types. The loss function, which measures the error between predicted and actual values, reached a low value of 0.645 after 200 epochs of training. This indicates that the model has learned to make precise predictions, and the reduction in loss over time signifies its improving performance.

A confusion matrix is used to evaluate the performance of a soil image classification model. It presents a summary of the model's predictions versus the actual class labels. Fig. 12 represents the confusion matrix for the classified soil.

Table 3 represents the performance evaluation of classified soil images. The performance metrics collectively demonstrate the effectiveness of the soil image classification model. High accuracy, recall, precision, specificity, and an F1 -score of 97.34% highlight the model's ability to accurately classify soil types. Additionally, low MAE, MSE, and RMSE values indicate that the model's predictions are close to the actual values, emphasizing its reliability in soil classification tasks.

4.2 Results regards to crop prediction

Crop prediction model, which leverages the ESO method for feature selection and the IPEA for classification, has yielded remarkable results. This combination of feature selection and classification techniques has proven to be highly effective in forecasting crop yields and

Table 4 Statistical summary of crop prediction.csv file

Features	Area	Production	Yield (Tonnes/ Hectare)	Precipitation	Relative humidity	Maximum temperature	Mnimum temperature	Mean temperature
Count	1480	1480	1480	1480	1480	1480	1480	1480
mean	603.023	594.8689	120.9034	197.9561	190.6973	157.3392	110.2473	120.5736
std	408.3657	408.378	93.29631	115.3601	107.4386	82.5934	63.77177	68.56517
min	0	0	0	0	0	0	0	0
25%	232.75	222.75	44	96.75	99	97	55.75	67
50%	592.5	582.5	84.5	199.5	192	157	107	114
75%	958.25	950.25	198.25	296	279.25	227.25	157	178.25
Max	1327	1320	347	419	397	305	259	256

optimizing crop recommendations. Table 4 represents the statistical summary of crop prediction.csv file.

Table 4 provides statistical summaries of various features related to agricultural data, including area, production, yield, precipitation, and more. The statistics presented include the count of data points, the mean (average) value, the standard deviation (a measure of data spread), minimum and maximum values, and percentiles that represent different points in the data distribution

Table 5 provides statistical summaries for various features related to agricultural data, including nutrient levels (N, P, K), temperature, humidity, pH, and rainfall. The statistics presented include the count of data points, the mean (average) value, the standard deviation (a measure of data spread), minimum and maximum values, and percentiles that represent different points in the data distribution. These statistics offer valuable insights into the characteristics of the dataset and involved in data analysis and decision-making processes. These patterns highlight how specific factors influence each other within the context of crop prediction.

The pairplot graph is a valuable tool for exploring data relationships and selecting features for crop prediction. It informs data-driven decisions and supports the optimization of crop recommendations, ultimately benefiting the agriculture and food production sectors. Fig. 13 represents the pairplots for selected features. The pairplot graph reveals patterns of correlation among the chosen features. Positive correlations are depicted as upward-sloping clusters of data points, while negative correlations are represented by downward-sloping clusters.

Fig. 14 represents the confusion matrix for predicted crops. The confusion matrix provides a detailed breakdown of the performance of our crop prediction model in classifying different crop types. It compares the model's predictions with the actual class labels, allowing us to evaluate the model's accuracy and its ability to correctly classify crops.

Fig. 15 represents the correlation matrix between different features of crop. The correlation matrix provides valuable insights into the relationships between various features used for crop prediction. It measures the degree of association between pairs of features, which is essential for understanding how these features interact and impact the predicted crop outcomes.

Fig. 16 represents the features of predicted crops. The selected feature aez_zone has above 4 count of predicted crops like groundnut, ragi, rice and sunflower. Similarly, for all selected features like Area, Yield, Annual_Rainfall, Minimum_Temperature and Mean_Temperature predicted count is displayed in the graph.

Table 5 Statistical summary of crop recommendation.csv file

Features	N	P	K	Temperature	Humidity	ph	Rainfall
Count	2200	2200	2200	2200	2200	2200	2200
mean	50.55182	53.36273	48.14909	25.61624	71.48178	6.46948	103.4637
std	36.91733	32.98588	50.64793	5.063749	22.26381	0.773938	54.95839
min	0	5	5	8.825675	14.25804	3.504752	20.21127
25%	21	28	20	22.76937	60.26195	5.971693	64.55169
50%	37	51	32	25.59869	80.47315	6.425045	94.86762
75%	84.25	68	49	28.56165	89.94877	6.923643	124.2675
max	140	145	205	43.67549	99.98188	9.935091	298.5601

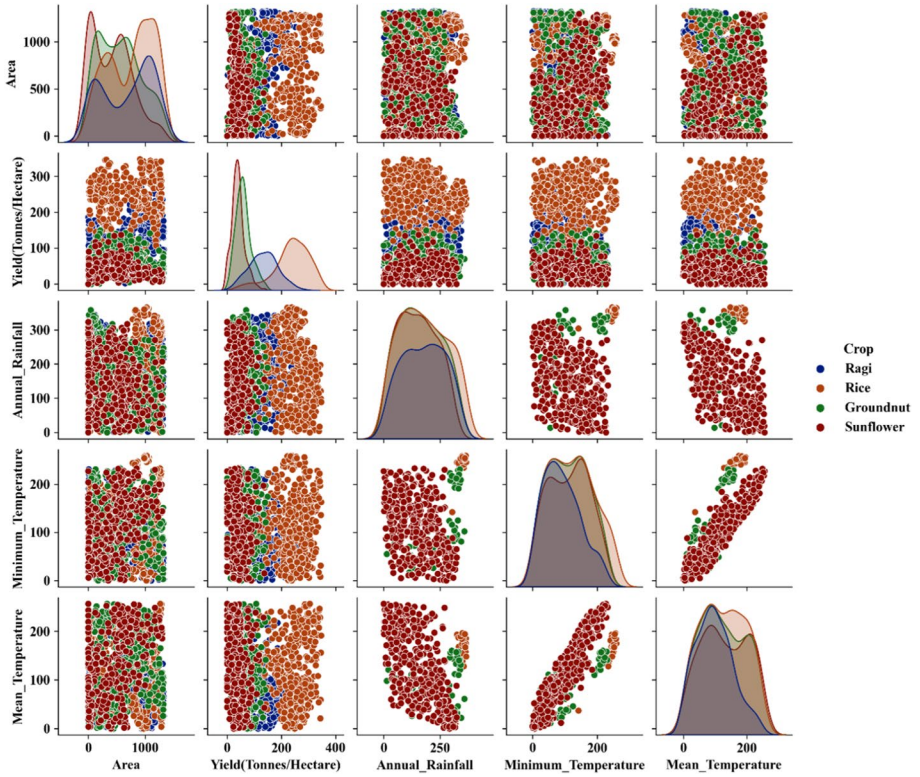

Fig. 13 Pairplot for selected features

Fig. 14 Confusion matrix for classified crops

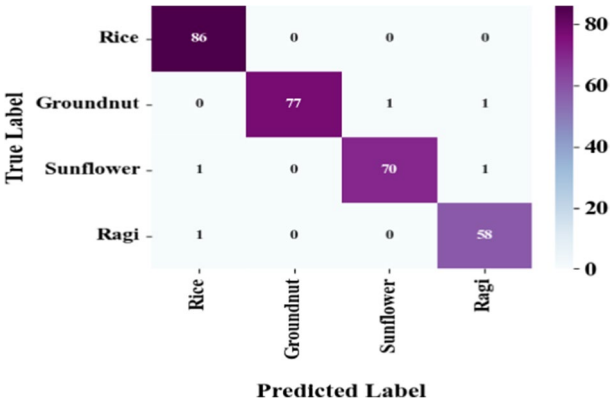

Table 6 presents evaluation metrics for different crops, including accuracy, precision, recall, specificity, and F1-score. These metrics are commonly used in classification tasks to assess the performance of a model. The crop classification model underwent extensive training for 200 epochs, during which it achieved exceptional performance. Figures 17 and 18 shows the accuracy and loss value of predicted crop during training

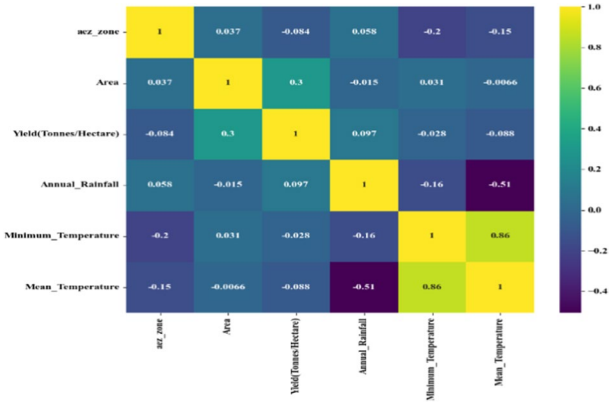

Fig. 15 Correlation matrix between different features

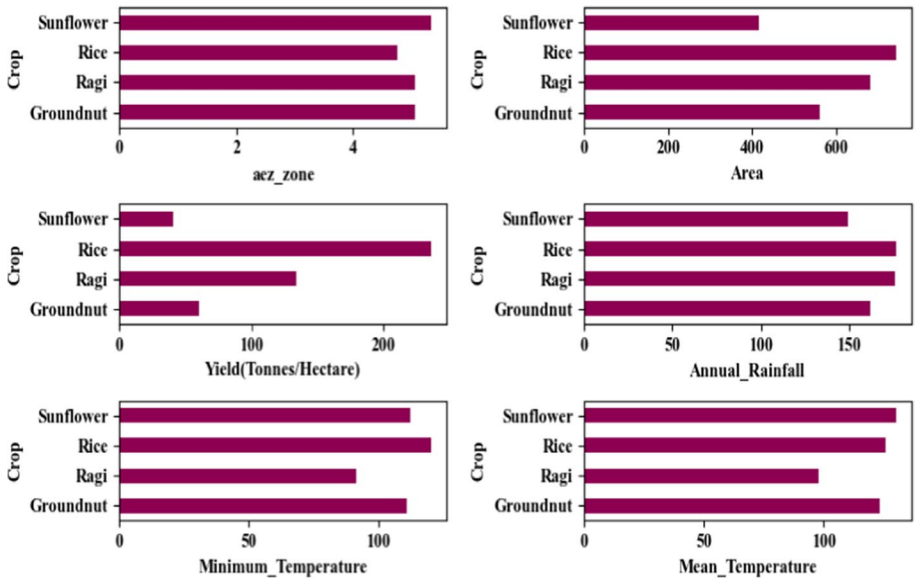

Fig. 16 Features of classified crops

Table 6 Overall performance of predicted crops

Crops	Evaluation metrics (%)				
	Accuracy	Precision	Recall	Specificity	F1-score
Rice	99.324324	97.727273	99.047619	99.047619	98.850575
Groundnut	99.324324	100.00000	97.468354	100.00000	98.717949
Sunflower	98.986486	98.591549	97.222222	99.553571	97.902098
Ragi	98.986486	96.666667	98.30585	99.156118	97.478992

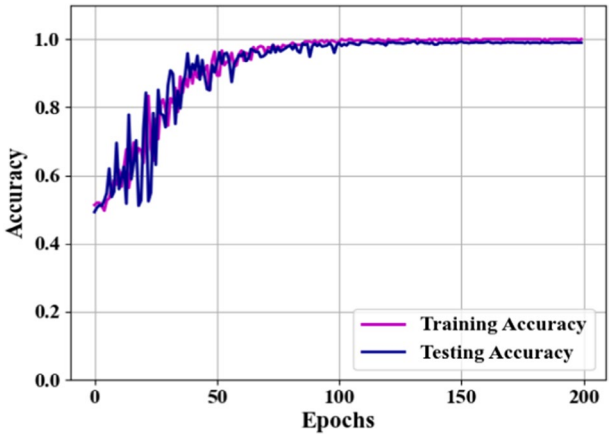

Fig. 17 Accuracy for classified crops

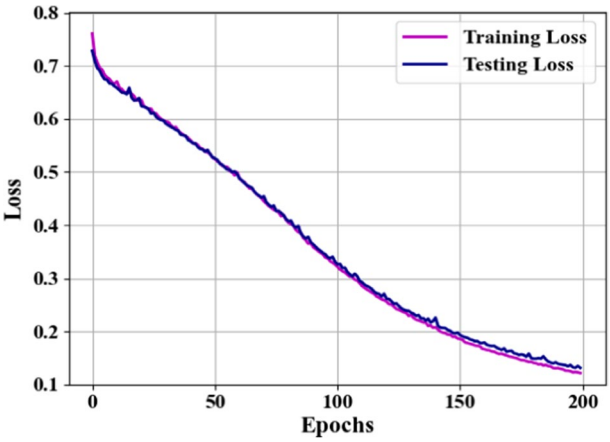

Fig. 18 Loss for classified crops with various epochs

The model demonstrated an impressive accuracy of 0.99, indicating that it correctly classified crops with a high degree of correctness. This high accuracy underscores the model's capability to make accurate predictions regarding different crop types.

The model achieved a low loss of 0.245 over the course of 200 epochs. Loss is a measure of the error between predicted and actual values, and a lower loss indicates that the model's predictions were consistently close to the true values.

Fig. 19 represents the convergence curve for the optimization method. The y-axis of the convergence curve represents the fitness value. In this case, the fitness value reached a commendable level of 0.25. The fitness value is a measure all that well the algorithm's solutions align with the desired outcome. Achieving a fitness value of 0.25 indicates a high level of optimization and effectiveness in crop classification. The x-axis signifies the number of iterations, and in this scenario, the algorithm underwent 100 iterations. Each iteration involves the exploration and refinement of solutions to improve the accuracy and reliability of crop classification.

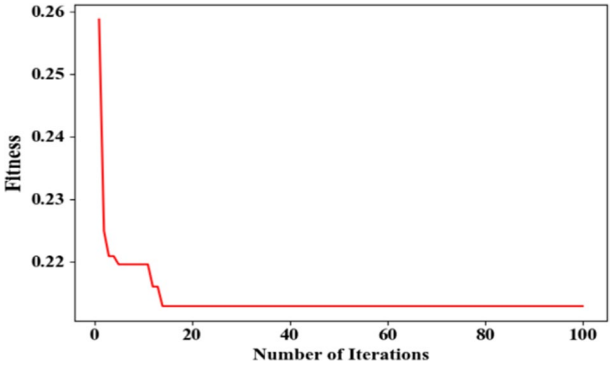

Fig. 19 Convergence curve for optimization method

4.3 Results regards multi crop recommendation

In multi-crop recommendation system, leverage a sophisticated fusion approach to combine information from two crucial sources: the classified soil data and the predicted crop data. The goal is to provide farmers and agricultural stakeholders with highly informed crop recommendations tailored to their specific soil conditions.

Fig. 20 represents the distribution of crop types as a result of the crop recommendation system's output. This visualization provides valuable insights into the diversity and composition of recommended crops based on various factors, including soil properties, climate conditions, and historical data.

Fig. 21 shows a visual summary of the selected features and their respective counts from the fused dataset. This visualization provides crucial insights into the most influential variables considered in analysis.

Fig. 22 presents a correlation matrix for the selected features from the fused dataset, specifically tailored for the recommendation system. This matrix offers valuable insights into the relationships between these features and informs the recommendation process.

Fig. 23 represents the framework of recommendation process. It includes the parameters like district name, ratio of nitrogen, phospherous, potassium, temperature, humidity, PH, rainfall and soil type. Fig. 24 represents the recommended crops for the entered parameters. It recommends the crops like jute, papaya, orange, muskmelon for the district Mandya and the soil type is clay.

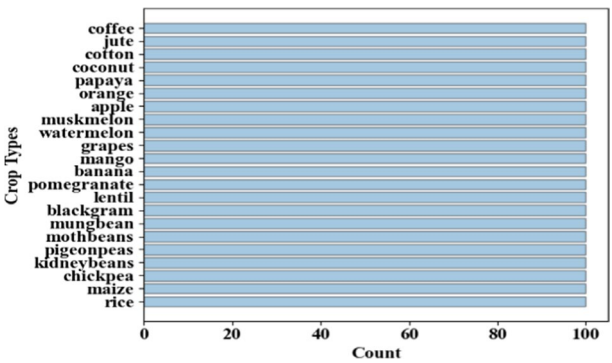

Fig. 20 Distribution crop type of recommended crops

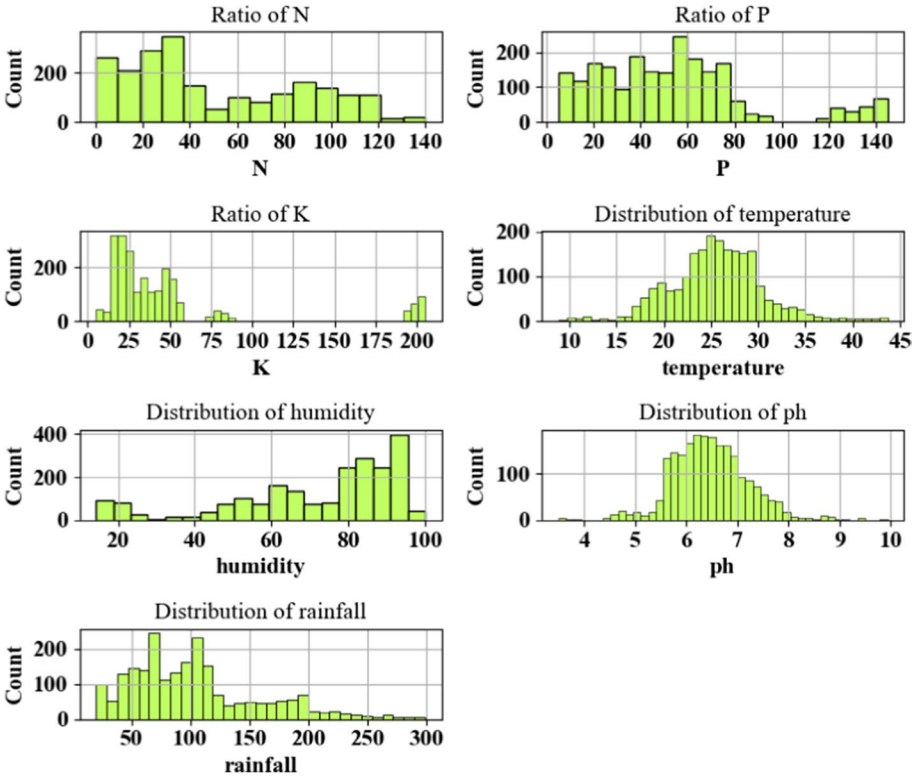

Fig. 21 Selected features and its count from fused dataset

Fig. 22 Correlation matrix of selected features

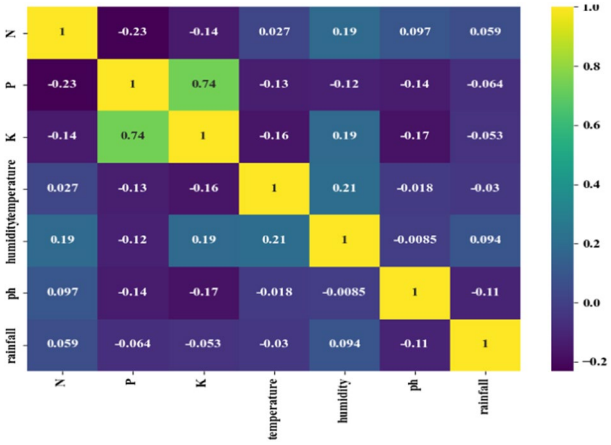

4.4 Statistical analysis for selected features

The experimental results are verified with statistical analysis like odds ratio and chi-square statistic, Table 7 represents the findings of statistical analysis.

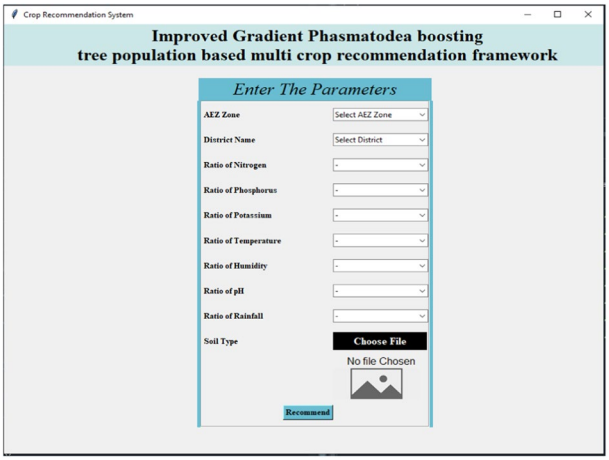

Fig. 23 Recommendation framework

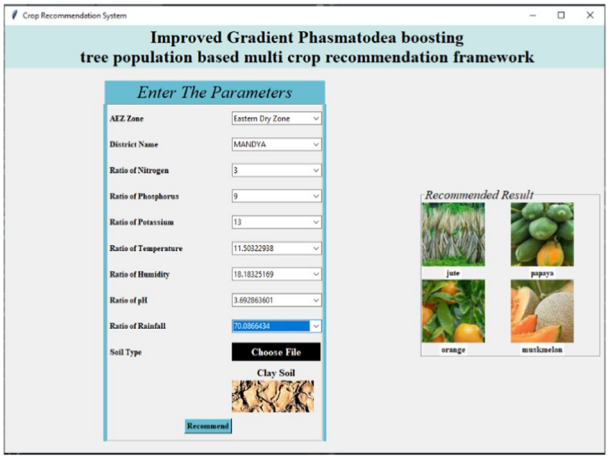

Fig. 24 Recommended results

Table 7 OR and Chi-square score for selected features

Selected features	Chi-square score	OR
aez_zone	36.903257	0.972
Area	9.167768	
Yield (Tonnes/Hectare)	0.027411	
Annual_Rainfall	0.599193	
Minimum_Temperature	2.906026	
Mean_Temperature	2.278377	

- Odds Ratio
- Odds Ratio (OR) measures the probability of a particular feature occurring in the positive class compared to the negative class. This statistical concept is founded on the premise that the distribution of features varies between instances associated with creditworthiness and those linked to credit risk. Mladenic applied odds ratio to select

relevant terms in text categorization. Eqn. (21) is the formula to express the Odds ratio function.

$$OR(d,s) = \log\frac{P(d|s)}{P(d|s)} \times \frac{1 - P(d|s)}{P(d|s)} \tag{21}$$

where, $OR(d,s)$ represents the odd ratio for the term d and class S; $P(d|s)$ represents the conditional probability of classes. Table 3 presents the Odds Ratio (OR) values. Specifically, the OR for selected features in the credit risk dataset is 0.975, for the credit risk analysis dataset, it is 0.983, and for the credit risk classification dataset, the OR values are 0.993 and 0.983.

- Chi-square Statistic
- It is used to evaluate the independence or association between two categorical variables. It is commonly applied to evaluate the relationship between predictor and target variable in CRA. Eqn. (22) shows the mathematical representation of chi-square statistic.

$$x^2 = \frac{\sum \left(O_{\_ij} - E\_ij\right)^2}{E\_ij} \tag{22}$$

where, x^2 represented as chi-square statistic, $O_{\_ij}$ denoted as the observed frequency in a particular cell of a contingency table for the i^{th} category of one variable and the j^{th} category of another variable and E_ij denoted as the expected frequency.

Table 7 shows the chi square sore of selected features like aez-zone, area, yield, annual-rainfall, minimum-temperature and mean-temperature. And obtained OR value is 0.972%

4.5 Comparison between classification and recommended methods

A comprehensive comparison between the classification methods is described in this section, which is used for soil analysis, and the recommended method, which assists in crop selection. Both methodologies play pivotal roles in optimizing agricultural practices, but they serve distinct purposes and operate at different stages of the farming process.

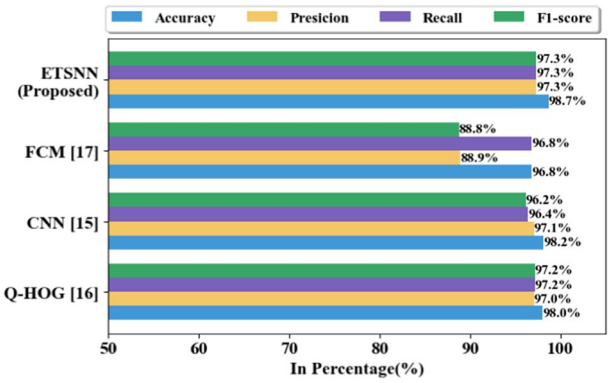

Fig. 25 Comparison for soil classification methods

Fig. 25 represents a comparative analysis of soil classification methods, including the existing methods, namely Q-HOG [16], CNN [15], and FCM [17], alongside proposed ETSNN method. This analysis sheds light on the performance of each method in terms of accuracy, precision, recall and F1-score. ETSNN achieves an impressive accuracy rate of 98.7% in soil classification. This exceptional performance featured to the ability of models to capture intricate spatiotemporal patterns in soil images.

Fig. 26 represents a comparative analysis of crop recommendation methods, including established approaches such as RFOERNN [21], Cap-DiBiL [22], and PSO-SVM [23], along with proposed ETSNN method. ETSNN capitalizes on both spatial and temporal features for improved accuracy. It achieves a remarkable accuracy rate of 99.7% in crop recommendation. This exceptional performance signifies ETSNN's ability to provide highly accurate crop suggestions to farmers.

The fusion of classified soil information and predicted crop data through a stacking-based fusion method significantly improved multi-crop recommendations. This approach empowered farmers with tailored insights, fostering sustainable and high-yield agricultural practices. It represented a valuable tool in modern agriculture, contributing to increased food production and efficient resource utilization. These results have significant implications for precision agriculture, environmental monitoring, and land management, where precise soil characterization is crucial for informed decision-making.

4.6 Case studies

Several motivational examples are provided in connection with the proposed approach.

Case Study 1: In a real-world application, farmers in a region with diverse soil and climate conditions used a multi-crop recommendation system for precision agriculture. Inputting location-specific soil properties, the system suggested various crops based on soil classification and predicted yields. Following the recommendations for a season, farmers implemented diverse crops suitable for their soil conditions, leading to increased overall crop yield. The adoption of recommended crops reduced reliance on synthetic inputs, as they were better suited to the soil, minimizing the need for excessive fertilizers or pesticides. This diverse crop selection contributed to sustainable agriculture, moving away from monoculture and promoting environmental conservation.

Case Study 2: Agricultural authorities in a district, facing challenges of inconsistent crop yields and soil degradation, initiated a government project to implement a multi-crop

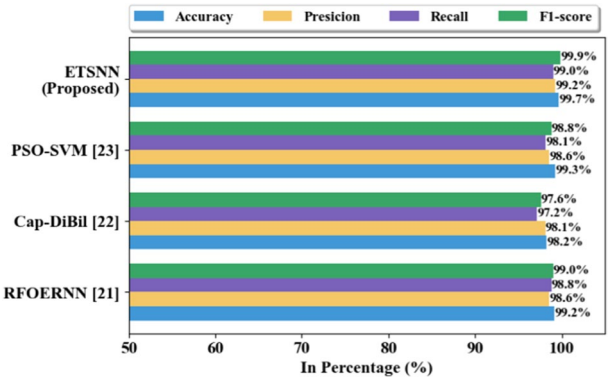

Fig. 26 Comparison for crop recommendation methods

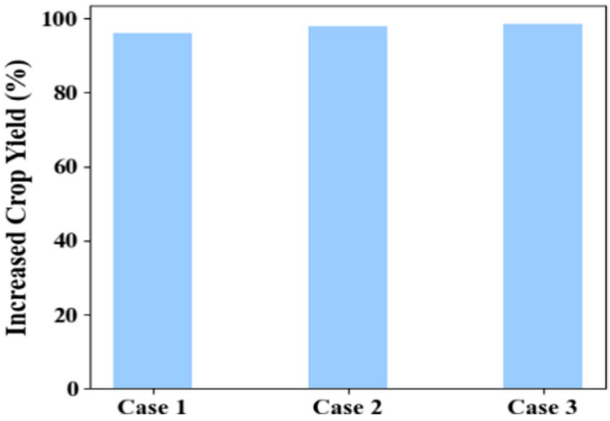

Fig. 27 Performance of crop yeild

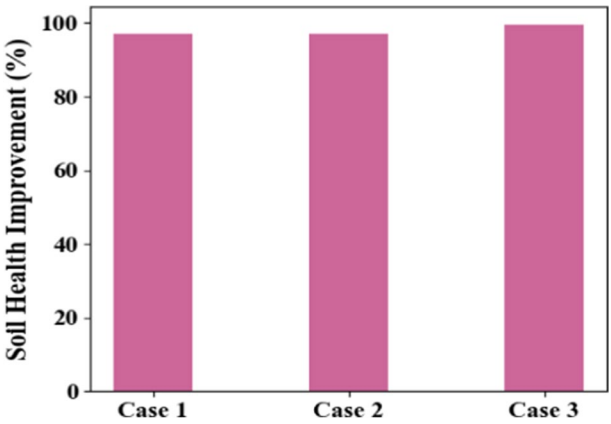

Fig. 28 Performance of soil health improvement

recommendation system. Integrated into a user-friendly interface for local farmers, the system's soil classification module identified soil types, enabling practices to improve soil health. The recommended diverse crops reduced mono-cropping risks, enhancing agricultural ecosystem resilience. The user interface enabled real-time input, empowering farmers to make informed decisions based on local soil conditions and environmental factors.

Case Study 3: An agricultural cooperative aimed to optimize collective crop selection for maximum productivity. Customizing the multi-crop recommendation system for collective input, it considered aggregated soil data and predicted yields for the entire group. The shared platform allowed cooperative members to input soil data and receive recommendations, optimizing crop selection. By choosing crops based on aggregated data, the cooperative achieved higher profitability, tailored to combined soil conditions. The system facilitated data-driven planning, enabling effective crop rotations and distribution for sustained agricultural success.

Figs. 27, 28 and 29 depict the achieved percentages of crop yield, soil health improvement, and profitability, showcasing a remarkable increase of over 95% across three distinct case scenarios. This substantial enhancement signifies the efficacy of the proposed multi-crop recommendation system. The significant rise in crop yield underscores the system's potential to optimize agricultural practices, ensuring greater food production. Improved

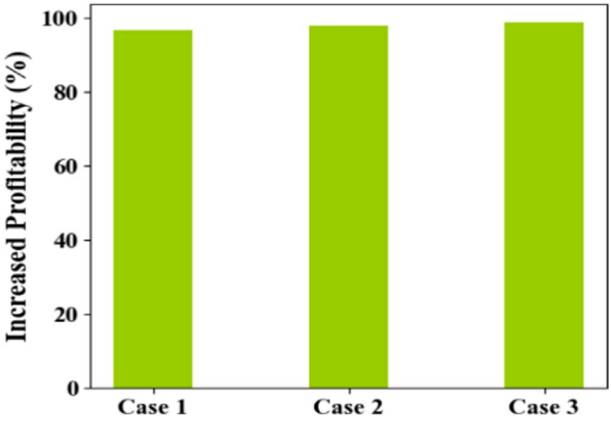

Fig. 29 Performance of increased profitability

soil health suggests sustainable cultivation practices, mitigating concerns related to soil degradation. The notable increase in profitability reaffirms the economic viability of the recommended crops. These findings underscore the system's substantial contribution to fostering sustainable agriculture, addressing key challenges, and enhancing overall agricultural outcomes.

5 Conclusion and future work

Improved gradient phasmatodea boosting tree population based multi crop recommendation framework is proposed to enhance agricultural decision-making, increase productivity and optimize resource utilization. ETSNN classification method 12.65% accurately predict the soil in first step and IPEA prediction method 15.31% accurately predict the crops in next step. Stacking based fusion approach is fused the two methods and recommends the multicrops robustly. The proposed approach is compared with existing methods and proved that the proposed recommended system predict the multicrops robustly. The proposed method is estimated with the help of several performances evaluating metrics mean absolute error, mean square error, accuracy, root mean square error, F1-score, recall, precision and specificity. The future of multicrop recommendation systems in agriculture holds promise for increased food production, resource conservation and climate resilience. Continuous research, innovation, and collaboration will be key in realizing these benefits and addressing the evolving challenges in agriculture.

Authors' contribution All the authors have contributed equally to the work.

Funding This research did not receive any specific grant from funding agencies in the public, commercial, or not-for-profit sectors.

Data availability Data sharing not applicable to this article as no datasets were generated or analysed during the current study.

Declarations

Ethical approval All applicable institutional and/or national guidelines for the care and use of animals were followed.

Informed consent For this type of analysis formal consent is not needed.

Disclosure of potential conflict of interest The authors declare that they have no potential conflict of interest.

References

1. Bakthavatchalam K, Karthik B, Thiruvengadam V, Muthal S, Jose D, Kotecha K, Varadarajan V (2022) IOT framework for measurement and precision agriculture: Predicting the crop using machine learning algorithms. Technol 10:13
2. Bali N, Singla A (2021) Deep learning based wheat crop yield prediction model in Punjab region of North India. Appl Artificial Intell 35:1304–1328
3. Sivanantham V, Sangeetha V, Alnuaim AA, Hatamleh WA, Anilkumar C, Hatamleh AA, Sweidan D (2022) Quantile correlative deep feedforward multilayer perceptron for crop yield prediction. Comput Electrical Eng 98:107696
4. Nischitha K, Vishwakarma D, Ashwini M, MR (2020) Crop prediction using machine learning approaches. Int J Eng Res. https://doi.org/10.17577/ijertv9is080029
5. Oikonomidis A, Catal C, Kassahun A (2022) Hybrid deep learning-based models for crop yield prediction. Appl Artificial Intell. https://doi.org/10.1080/08839514.2022.2031823
6. Elavarasan D, Vincent PM (2020) Crop yield prediction using deep reinforcement learning model for Sustainable Agrarian Applications. IEEE Access 8:86886–86901
7. Jhajharia K, Mathur P (2023) Prediction of crop yield using satellite vegetation indices combined with machine learning approaches. Adv Space Res 72:3998–4007
8. Olofintuyi SS, Olajubu EA, Olanike D (2023) An ensemble deep learning approach for predicting cocoa yield. Heliyon. https://doi.org/10.1016/j.heliyon.2023.e15245
9. Suruliandi A, Mariammal G, Raja SP (2021) Crop prediction based on soil and environmental characteristics using feature selection techniques. Mathe Comput Model Dyn Syst 27:117–140
10. Raja SP, Sawicka B, Stamenkovic Z, Mariammal G (2022) Crop prediction based on characteristics of the agricultural environment using various feature selection techniques and classifiers. IEEE Access 10:23625–23641
11. Durai SK, Shamili MD (2022) Smart farming using machine learning and deep learning techniques. Dec Analytics J 3:100041
12. Thilakarathne NN, Bakar MS, Abas PE, Yassin H (2022) A cloud enabled crop recommendation platform for machine learning-driven precision farming. Sensors 22:6299
13. Madhuri J, Indiramma M (2021) Artificial neural networks based integrated crop recommendation system using soil and climatic parameters. Indian J Sci Technol 14:1587–1597
14. Kiruthika S, Karthika D (2023) IOT-based professional crop recommendation system using a weight-based long-term memory approach. Measurement: Sensors 27:100722
15. Lanjewar MG, Gurav OL (2022) Convolutional neural networks based classifications of soil images. Multimed Tools Appl 81:10313–10336
16. Uddin M, Hassan MdR (2022) A novel feature based algorithm for soil type classification. Comp Intell Syst 8:3377–3393
17. Kumar Dutta A, Albagory Y, Al Faraj M, Alsanea M, Rahaman Wahab Sait A (2023) Cat swarm with fuzzy cognitive maps for automated soil classification. Comput Syst Sci Eng 44:1419–1432
18. Kumar S, Sharma B, Sharma VK, Poonia RC (2021) Automated soil prediction using bag-of-features and chaotic spider monkey optimization algorithm. Evolut intell 14:293–304
19. Barman U, Choudhury RD (2020) Soil texture classification using multi class support vector machine. Info Process Agric 7:318–332
20. Kamath P, Patil P, Shrilatha S, Sushma SS (2021) Crop yield forecasting using data mining. Global Trans Proc 2:402–407
21. Gopi PS, Karthikeyan M (2023) Red fox optimization with ensemble recurrent neural network for crop recommendation and yield prediction model. Multimed Tools Appl. https://doi.org/10.1007/s11042-023-16113-2
22. Munaganuri RK, Rao YN (2023) Cap-Dibil: An automated model for crop water requirement prediction and suitable crop recommendation in agriculture. Environ Res Commun 5:095016
23. Gupta S, Geetha A, Sankaran KS, Zamani AS, Ritonga M, Raj R, Ray S, Mohammed HS (2022) Machine learning- and feature selection-enabled framework for accurate crop yield prediction. J Food Quality 2022:1–7

24. Xia Z, Qiao T, Xu M, Wu X, Han L, Chen Y (2022) Deepfake video detection based on Mesonet with preprocessing module. Symmetry 14:939
25. Liu F, Zhao R (2022) Enhancing spiking neural networks with hybrid top-down attention. Front Neurosci. https://doi.org/10.3389/fnins.2022.949142
26. Alahmer H, Alahmer A, Alamayreh MI, Alrbai M, Al-Rbaihat R, Al-Manea A, Alkhazaleh R (2023) Optimal water addition in emulsion diesel fuel using machine learning and sea-horse optimizer to minimize exhaust pollutants from diesel engine. Atmosphere 14:449
27. Wu T-Y, Li H, Chu S-C (2023) CPPE: An improved phasmatodea population evolution algorithm with chaotic maps. Mathe 11:1977

Authors and Affiliations

Chetan R[1,2] · D. V. Ashoka[3] · Ajay Prakash B[4]

✉ Chetan R
chetanr@jssateb.ac.in

D. V. Ashoka
dvashoka@jssateb.ac.in

Ajay Prakash B
ajayprakas@gmail.com

[1] Department of Computer Science and Engineering, JSS Academy of Technical Education, Visvesvaraya Technological University, Karnataka, India

[2] Department of Information Science, JSS Academy of Technical Education, Visvesvaraya Technological University, Karnataka, India

[3] Department of Information Science and Engineering, JSS Academy of Technical Education, Visvesvaraya Technological University, Karnataka, India

[4] Department of Artificial Intelligence and Machine Learning, Dr. Ambedkar Institute of Technology, Visvesvaraya Technological University, Karnataka, India